Journal Pre-proof

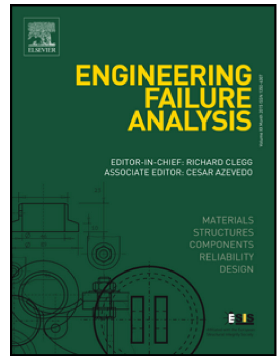


# Numerical simulation of fatigue crack propagation: A case study of defected steam pipeline

B. Aleksić, A. Grbović, Lj. Milović, A. Hemer, V. Aleksić

PII: S1350-6307(19)30423-6

DOI: https://doi.org/10.1016/j.engfailanal.2019.104165

Reference: EFA 104165

To appear in: *Engineering Failure Analysis*

Received date: 21 March 2019

Revised date: 15 July 2019

Accepted date: 28 August 2019

Please cite this article as: B. Aleksić, A. Grbović, L. Milović, et al., Numerical simulation of fatigue crack propagation: A case study of defected steam pipeline, *Engineering Failure Analysis*(2018), https://doi.org/10.1016/j.engfailanal.2019.104165

# Numerical simulation of fatigue crack propagation: A case study of defected steam pipeline

B. Aleksić [a,*], A. Grbović [b], Lj. Milović [c], A. Hemer [c] and V. Aleksić [d]

[a] *University of Belgrade, Innovation Centre, Faculty of Technology and Metallurgy, Karnegijeva 4, 11120 Belgrade, Serbia*

[b] *University of Belgrade, Faculty of Mechanical Engineering, Kraljice Marije 16, 11120 Belgrade, Serbia*

[c] *University of Belgrade, Faculty of Technology and Metallurgy, Karnegijeva 4, 11120 Belgrade, Serbia*

[d] *Institute for testing of materials- IMS Institute, Bulevar vojvode Mišića 43, 11000 Belgrade, Serbia*

**Abstract**

In order to prevent the premature failure of steam pipeline produced of molybdenum-vanadium steel, the experimental tests were performed to measure fracture toughness and to determine the mechanical behaviour of cracked pipes. A finite element method was used to calculate the fracture behaviour of the pressurized pipeline made of 14MoV6-3 steel based on the *J*-integral computation. The *J-R* curves were experimentally obtained by the elastic unloading compliance method for the single edge notched bend specimens and compared with those obtained using finite element method.

A two dimensional finite element analysis was performed in Ansys Workbench software to determine the stress distribution and calculate *J*-integral values for the selected specimen geometry. Special attention was paid to the influence of applied boundary conditions on the accuracy of *J*-integral values, as well as to the influence of mesh density. It is shown that numerically obtained *J*-values significantly depend on the number of nodes used to apply displacements. However, if recommendations proposed in this paper are implemented, the accuracy of calculated values is satisfactory and successful failure analysis can be carried out. This approach can be useful in engineering applications where time saving and costs reducing are required.

*Keywords*: Steam pipelines failures; *J*-integral; *J-R* curve; Finite element method

## 1. Introduction

The molybdenum-vanadium steel 14MoV6-3 (EN 1.7715) is used for manufacturing of boilers and steam pipelines designed for steam temperatures up to 580 °C. Since 1970s the steel grade 14MoV6-3 has been used in thermal power plants in Serbia for the manufacturing of equipment designed to operate at elevated temperatures. Operational experiences with plant components' made of this particular grade are beyond expectation because most of the examined elements have exceeded their assessed operating life of 100,000 hours under operational conditions of steam temperature of 540 °C and steam pressure of 4.5 MPa, [1-6].

Still premature failures of steam pipelines manufactured from 14MoV6-3 steel, occurs. Failures caused by simultaneous effect of temperature, fatigue loading and aggressive environment are usually manifested as through-the-thickness cracks and they lead to the leakage-before-break of pipelines. Instead of repairing existing damaged pipelines made of 14MoV6-3 steel, engineers prefer to replace them with a new ones made of different steel grades. Better understanding of the 14MoV6-3 steel behaviour can be of assistance in reducing unexpected service interruption and improve the reliability and safety of thermal power plants, [3].

The local approach to fracture has been developed for full understanding of the fracture mechanism. The approach is a combination of the theory, experiment and numerical solution, which enables less conservative assessment of the significance of fractures and residual stresses [2, 3, 7].

Steam pipelines belong to highly reliable structures, and for this reason, steam pipeline, i.e. the material of the steam pipeline, together with its welded joints, undergoes damage that is accumulated during exploitation and can lead to fracture. The basic property of the steel for steam pipelines is resistance to creep and fracture in a designed time.

Material crack resistance can be assessed by fracture mechanics parameters: stress intensity factor for mode one of loading $K_I$, crack-tip opening displacement $\delta$ and $J$-integral. Their critical values $K_{Ic}$, $\delta_C$ and $J_{Ic}$, can be used as properties of the homogeneous material, [8-11].

Several authors have studied pipe fracture problems by means of experimental testing and numerical simulation in order to assess the mechanical integrity, taking into account different crack shapes, [12-14]. In experimental mesurements attention is most often directed to mesurement of the fracture initiation resistance, $J_{IC}$ and $J$-$R$ curve. The $J$-$R$ curve is experimentally determined using a single specimen method, the method that follows elastic deformation together with measured crack mouth opening. Along with the development of computer science technology, the demanding experimental procedures for determining $J$-integral were replaced by numerical methods. The finite element method (FEM) was extensively applied in this subject, and some works on this topic include two dimensional FE analysis of specimen stress with short cracks of SEN(B) sample [15], with a proposed equation for $J$-assessment [16].

In this paper the methodology of calculation of critical values of the $J$-integral, $J_{IC}$ is presented. The main idea of the present work is to determine experimental $J$-integral, where critical values of the $J$-integral are compared with the values obtained by using FEM. FEM model was defined on the basis of experimental conditions in program Ansys Workbench, and special attention was paid on the influence of the mesh density as well as of the applied boundary conditions on the accuracy of obtained $J$-integral values.

## 2. Material

Steel grade 14MoV6-3 is classified as low-carbon steel microalloyed with chromium, molybdenum and vanadium. It is delivered in normalized and tempered condition. The chemical composition of the investigated material is given in Table 1.

Table 1. Chemical composition of as-received steel, %wt.

| C | Si | Mn | P | S | Al | Cr | Mo | V |
|---|---|---|---|---|---|---|---|---|
| 0.12 | 0.37 | 0.65 | 0.01 | 0.01 | 0.004 | 1.042 | 0.24 | 0.16 |

For tensile and impact testing, the specimens were taken from the pipe of outside diameter 609 mm and of wall thickness 25 mm. Mechanical properties of material used for further investigation are given in Table 2.

Table 2. Mechanical properties of tested material.

| Elasticity modulus<br>$E$, GPa | Yield stress<br>$R_{p0.2}$, MPa | Tensile strength<br>$R_m$, MPa | Elongation<br>$A$, % | Total impact energy,<br>$E_{tot}$, J | Poisson's coefficient<br>$\nu$ |
|---|---|---|---|---|---|
| 190 | 320 | 460 | 27.19 | 99.12 | 0.3 |

## 3. *J*-integral calculation

The investigation of fracture mechanics parameters, in this case $J_{Ic}$, was conducted on a 14MoV6-3 steel specimen in the presence of a crack-type defect, as the most dangerous of all the defects in the structural materials.

Fracture toughness testing were performed using single edge notched bend SEN(B) specimen of 17.6 mm thickness shown in Fig.1, according the standard ASTM E1820 [10]. The distance between the support rollers was 128 mm.

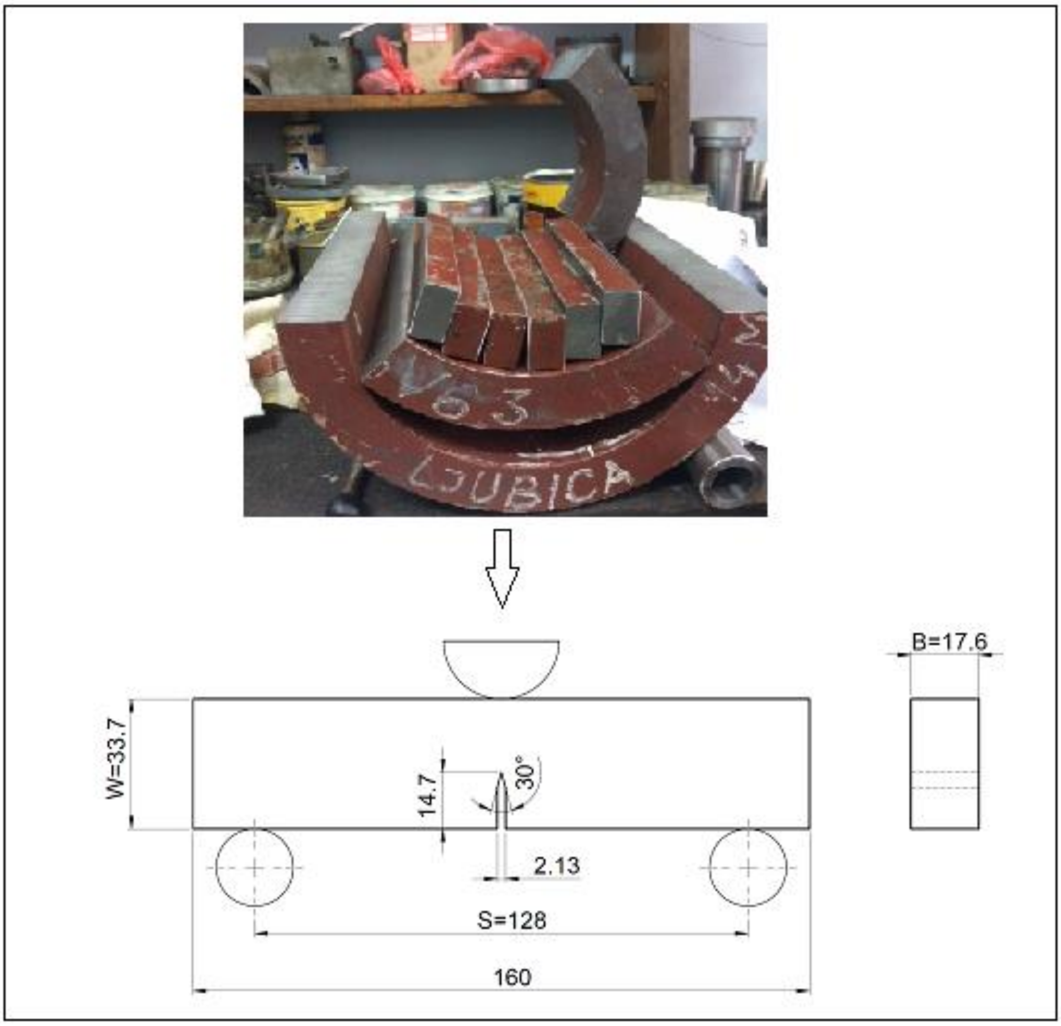


Fig. 1. Test specimen from the pipe shown in the photograph (all dimensions in millimetres)

Fracture toughness $K_{Ic}$, a measure of fracture toughness $J_{Ic}$, is determined based on *J*-integral critical value, by testing according to ASTM E899-06 standard [8]:

$$K_{Ic} = \sqrt{\frac{J_{Ic} \cdot E}{1-\nu^2}} \quad (1)$$

For the determination of the *J*-integral, a single specimen testing method by successive partial unloading was applied. By data pairs applied force, *F*, crack opening displacement, $\delta$, the points of basic relationship curve were obtained, Fig. 2a.

The procedure for the determination of critical value, as measure of the fracture toughness, $J_{Ic}$, requires the design of *J-R* curve, shown in Fig. 2b, in which the crack growth is determined based on changing in compliance.

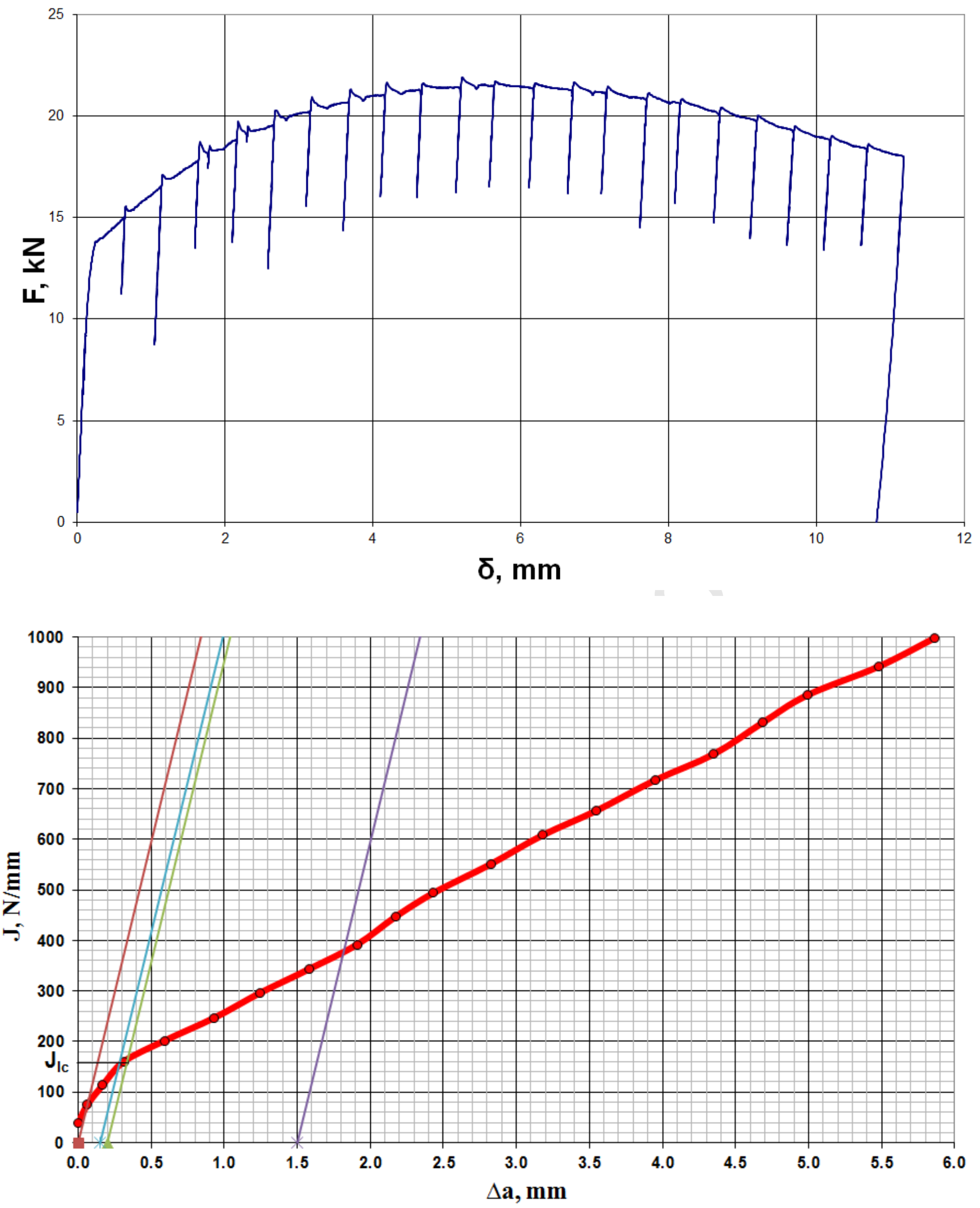


Fig. 2. Diagrams $F-\delta$ (a) and $J-\Delta a$ for the tested specimen (b)

In a single specimen test, the specimen is unloaded in intervals to about 30% of the actually attained level of force chosen by experience with this type of material. Based on the change of line slope of the compliance, $C$, with crack extension, the crack increase, $\Delta a$, between two successive unloading, corresponding to the attained value of force, is determined as [10]:

$$\Delta a_i = \Delta a_{i-1} + \left(\frac{b_{i-1}}{\eta_{i-1}}\right)\cdot\left(\frac{C_i - C_{i-1}}{C_{i-1}}\right) \qquad (2)$$

The next steps are determination of critical value, $J_{Ic}$, and use of this value in Eq. (1) for the calculation of the fracture toughness, $K_{Ic}$, according the single specimen compliance method.

The values given in Table 3, critical $J$-integral, $J_{Ic}$, and the values of critical stress intensity factor, $K_{Ic}$, were obtained from the diagram $J$-$\Delta a$ shown in Fig. 2b.

Table 3. $J_{Ic}$ and $K_{Ic}$. experimental values

| Critical J-integral $J_{Ic}$, N/mm | Critical stress intensity factor, $K_{Ic}$, MPa·√mm |
|---|---|
| 158 | 1810 |

## 4. Numerical *J*-integral Calculation

*J*-integral calculation is technique used to evaluate the intensity of the crack tip fields and correlate the initiation of crack growth in solids experiencing plastic deformation. It is well known that determination of *J* values under combined thermo-mechanical loading is not an easy task and that numerical method, such as FEM, is the most efficient tool for such a calculation. On the other hand, even with the use of FEM precise calculation of field quantities at nodes close to the crack tip is difficult. For this reason, finite area (or volume) domain integrals have been introduced for the computation of the *J* values and the virtual crack extension (VCE) technique is now generally used for this purpose.

In Ansys Workbench software used in this research, the *J*-integral evaluation is based on the domain integral method proposed in [17]. In a case of two-dimensional problems, the domain integration formulation applies area integration, while for three-dimensional problems volume integration is used. Area and volume integrals offer much better accuracy than contour/surface integral and are much easier to implement. In case of testing SEN(B) specimen, it is not necessary to develop three-dimensional finite element model for *J*-integral calculations because the more simple integration area is used. For a two-dimensional problem, the domain expression for the energy release rate is given by:

$$J = \int_A \left[ \sigma_{ij} \frac{\partial u_j}{\partial x_1} - W \delta_{1i} \right] \frac{\partial q1}{\partial x_i} dA + \int_A \alpha \sigma_{ii} \frac{\partial \theta}{\partial x_1} q_1 dA - \int_A \sigma_{ij} \frac{\partial \varepsilon^0_{ij}}{\partial x_1} q_1 dA - \int_C t_i u_{i,1} q_1 dC \quad (3)$$

where: $\sigma_{ij}$ is stress tensor, $u_j$ – displacement vector, $W$ – strain energy density, $\delta_{1i}$ – Kronecker delta, $x_i$ - local coordinate axis, $q$ – crack-extension vector, α – coefficient of thermal expansion, $\theta$ – temperature (relative to the ambient temperature), $\varepsilon^0_{ij}$ – initial strain tensor, $t_i$ – crack face traction, $A$ – integration domain, and $C$ – crack faces upon which tractions act.

In the absence of thermal strain and crack face traction, equation (3) reduces to:

$$J = \int_A \left\{ \left[ \sigma_{ij} \frac{\partial u_j}{\partial x_1} - W \delta_{1i} \right] \frac{\partial q1}{\partial x_i} - \sigma ij \frac{\partial \varepsilon^0_{ij}}{\partial x_1} q_1 \right\} dA \quad (4)$$

while in the absence of body force, equation 4 reduces to

$$J = \int_A \left\{ \left[ \sigma_{ij} \frac{\partial u_j}{\partial x_1} - W \delta_{1i} \right] \frac{\partial q1}{\partial x_i} \right\} dA \quad (5)$$

Similarly to the path-independency of *J*-integral, equation 5 shows the domain-independency, in other words independency of *J*-evaluation from the domain choice which is usually dictated by generated FE mesh. In a case when all loads are presented (body force, thermal strain and crack face traction), in order to use equation 5, the domain must include the region around crack tip.

The direction of crack-extension vector $q$ is the $x$-axis of the local coordinate system ahead of the crack tip. The $q$ vector is set to be zero at all nodes along the contour $\Gamma$, as well as a unit vector for all nodes inside $\Gamma$, except the mid-side nodes that are directly connected to the contour $\Gamma$. In Ansys Workbench, these nodes with a unit $q$ vector are referred as VCE nodes. These nodes are among the most important inputs required for the evaluation of $J$.

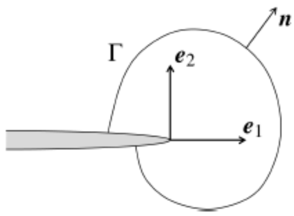


Fig. 3. Contour $\Gamma$ and coordinate system in the crack tip

For a two-dimensional crack problem, the crack-tip node component usually contains one node and the first contour for the integration area is evaluated over the elements associated with the crack-tip node component. In the next step, the new integration area is formed over the finite elements adjacent to the elements in the first contour, and so on. It is important, for the sake of accuracy, that elements inside the integration contour never reach the outer boundary of FE model. Moreover, fracture calculations rely on the element nodal connectivity order; so, it is important in Ansys Workbench to keep the middle nodes in the element nodal connectivity for the higher-order elements. The use of sweeping meshes along the crack fronts in three-dimensional modelling is highly recommended, while in case of two-dimensional problems, finer mesh in the near field around the crack tip is necessary.

In numerical simulations presented in this paper, all above-mentioned recommendations have been adopted. Finally, the influence of boundary conditions on the accuracy of calculated $J$ values was investigated.

### 4.1. Finite Element Model

In CATIA v5 software, the developing of appropriate FE model for $J$ values calculation on two-dimensional geometry of SEN(B) specimen has been defined, Fig. 4a. Since very fine mesh is needed in the vicinity of the crack tip, 40 sector-like surfaces were created around the tip, Fig. 4b, to provide the fine mesh generation.

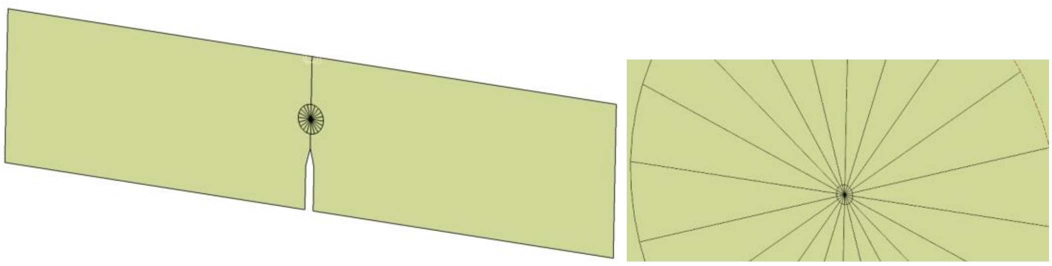

(a) (b)

Fig. 4. Geometry of SEN(B ) specimen (a) and detail around the crack tip (b) as created in CATIA v5

In total, five geometries, similar to one shown in Fig. 4, have been created and each had different crack-tip-to-bottom-edge distance: $d_1$ = 16.830 mm, $d_2$ = 18.074

mm, $d_3$ = 20.009 mm, $d_4$ = 21.821 mm and $d_5$ = 23.104 mm (initial distance $d$ = 14.70 mm is shown in Fig.1). These five distances correspond to distances measured in experiment with SEN(B) specimen. After importing geometries to Ansys Workbench, meshes were created with $n_1$ = 5864, $n_2$ = 6072, $n_3$ = 5956, $n_4$ = 6292 and $n_5$ = 6224 finite elements of type PLANE183. This is higher order, two-dimensional 8-node or 6-node element that has quadratic displacement behaviour suitable for irregular meshes modelling. PLANE183 should be used in cases of plane stress, plane strain and generalized plane strain and has two DOFs – translations in the nodal $x$ and $y$ directions – at each node. However, for the axisymmetric problems that include torsion, the element has three DOFs at each node: rotation in the nodal $y$ direction is added to previously mentioned two. Fig. 5 shows finer mesh around the crack tip for model with 20 mm distance from the tip to the bottom edge of specimen. Thickness of the FE model of specimen was set to $t$ = 17.60 mm.

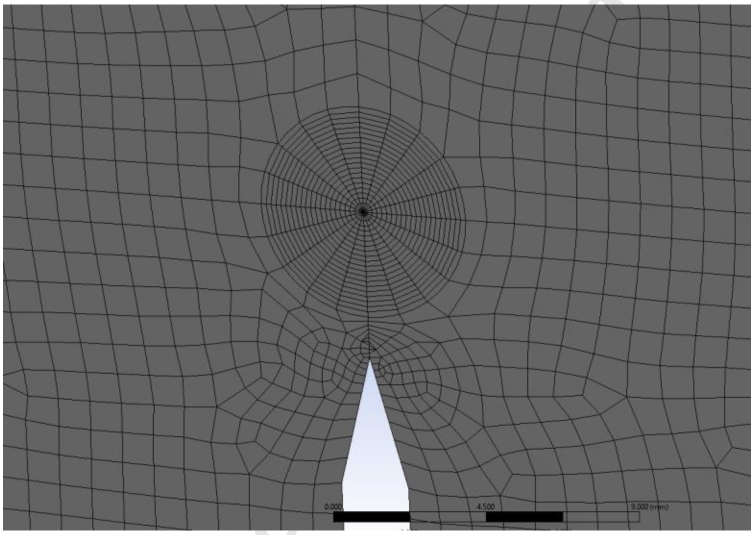

Fig. 5. Finer mesh around the crack tip (element type PLANE183)

Element PLANE183, among all other capabilities such as hyperelasticity, creep and stress stiffening, has plasticity, necessary for accurate $J$ calculations. Plastic behaviour of 14MoV6-3 steel was examined in experiment and then, in Ansys Workbench, constitutive behaviour was adopted based on experimental values, assuming the von Mises yield criterion with bilinear isotropic hardening, Fig. 6, similar to that presented in [18]. For linear elastic materials, the $J$-integral is a measure of energy; therefore, the relatively accurate $J$ values can be obtained even with coarse mesh, but this often results in inaccurate calculation of stress/displacement fields around the crack tip [19].

This fact was proved when calculations were carried out on FE models with coarse mesh obtained from the same geometry, Fig. 4. To be specific, FE mesh shown in Fig. 5 was generated after several trials and adjustments, and for initial calculations, the mesh with approximately 3000 nodes was used. Results obtained with both meshes were afterward compared and it was found that coarse mesh provided higher $J$ values. Difference between the values was on average 15% (see Fig. 10 in section Results and Discussion); therefore, it was decided to use models with finer mesh since they provided results closer to experimental values.

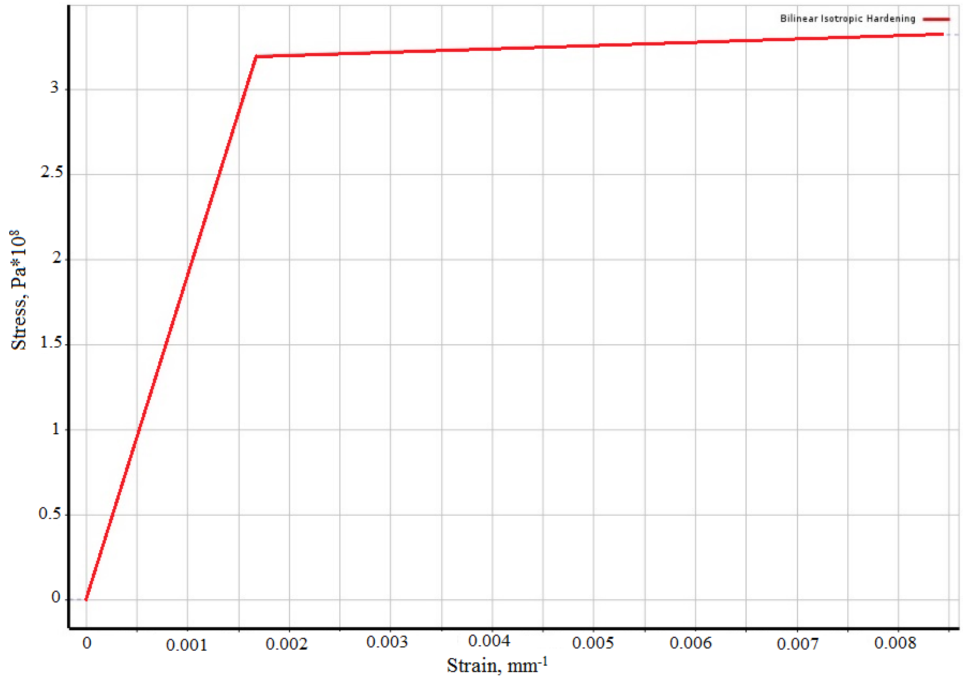


Fig. 6. Mathematical model used to describe the plastic behaviour of 14MoV6-3

Values for the force measured in experiment with SEN(B) specimen for five characteristic distances (from $d_1$ = 16.830 mm to $d_1$ = 23.104 mm) were $F_1$ = 15.250 kN, $F_2$ = 20.700 kN, $F_3$ = 21.200 kN, $F_4$ = 15.250 kN and $F_5$ =18.350 kN. A variable force over time was the reason why five FE models were used in simulations instead of one. Automatic crack growth, from initial to final length, can be completely simulated in Ansys Workbench and corresponding *J* values can be assessed using recently introduced **S**eparating **M**orphing and **A**daptive *R*e-meshing **T**echnology (SMART) [20]. SMART updates the mesh from crack-geometry changes due to crack growth automatically at each solution step and provides *J* solutions for every newly defined position of the crack tip. Unfortunately, multiple loading steps are yet not supported, and as a consequence, several FE models with different crack lengths must be used when the force is not static.

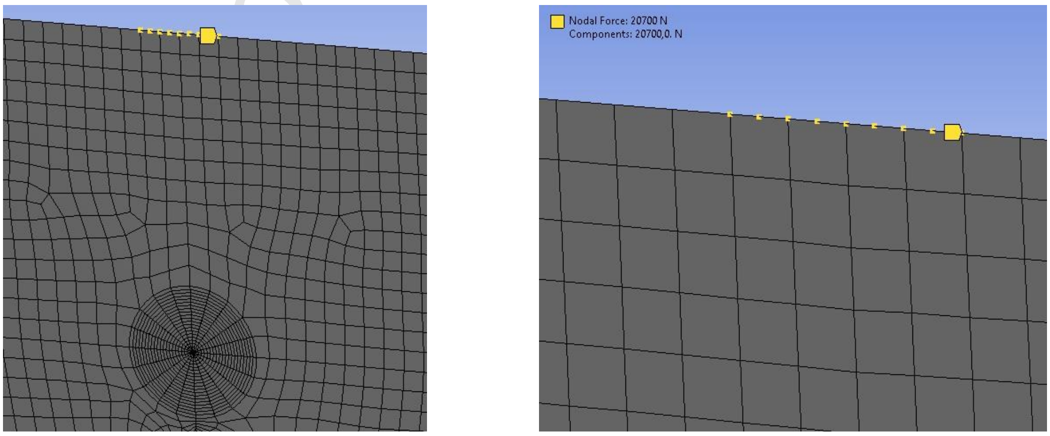


(a) (b)

Fig. 7. Forces were applied directly above the crack tip (a), at exactly 9 nine nodes (b)

Forces $F_1$ to $F_5$ were applied as nodal loads in positive *x* direction (downward, see red arrow in Fig. 7a) at exactly 9 nodes of quadratic finite elements above the crack tip. As can be seen in Fig. 7b, mid-side nodes have also been selected and force values associated with nodes were split into nine parts to introduce adequate boundary conditions. Distance between the first and the ninth node was approximately equal to the diameter of support roller.

Finally, boundary conditions that would consider position and the effect of support rollers had to be defined. Theoretically, contact between the support roller and the specimen is defined along a line (or in a case of two-dimensional FE model – at a single node), but in reality – due to material elasticity and high values of forces applied – contact between the support roller and the specimen is of surface-to-surface type.

This implies that for two-dimensional FE model of SEN(B) specimen more than one node must be constrained in order to faithfully simulate experimental conditions. Choice of the constrained nodes number is challenging task, because it is reasonable to assume that area of the surface in contact between two bodies changes over time; as a consequence, nodes numbers to be selected in two-dimensional simulation varies with crack length. Therefore, dozen simulations have been performed in this research to identify the nodes numbers that should be selected at positions of support rollers in order to get $J$ values for different crack lengths comparable to those obtained in experiment.

In first few simulations, only one node was selected at each of theoretical contacts between specimen and support rollers. Distance between these nodes was exactly 128 mm (the span between supports should be $s = 4 \cdot W$). In next simulations number of nodes selected at supports was gradually increased ($n$ = 3, 5, 7, 9, 11, 13 and 15), but the distance between central nodes was kept constant: $d$ = 128 mm. For all nodes at support on one side of the specimen displacements in $x$ and $y$ direction were restricted, while for nodes on the other support only displacement in $y$ direction was not allowed. Number of nodes at which the load is applied was also varied, but no considerable influence on calculated $J$ values was found.

## 5. Results and discussion

The force changes during the experiment, and therefore numerical analysis involved five characteristic crack lengths with five corresponding forces, applied on five different FE models.

Calculations have proved that a constant number of nodes cannot be used for supports in all five models. On the other hand, number of nodes used to apply the force does not affect much the values of calculated $J$-integral (as can be seen in Table 4) since they vary between 3 and 5%, but the differences in $J$ values for different numbers of nodes used to apply displacements are considerable. Higher values of applied force demand greater number of nodes to be selected, which is expected since the contact area between the support rollers and the specimen is increasing due to specimen's elastic deformation.

In the beginning, when the force value is the smallest ($F_1$ = 15.250 kN), contact area between the support rollers and the specimen is smallest too, and even theoretical one-point force or contact can be used, since FE analysis shows the best match with experimental data when one node is selected for each support and one node for force (Table 4, $d_1$ = 16.830 mm). Taking more nodes than one in this case leads to less accurate results. As the force increases elastic deformation increases and more nodes must be selected for applying the displacements, and the best matches are obtained when the number of nodes in supports is $n$ = 13 ($F_2$ = 20.700 kN) and $n$ = 15 ($F_3$ = 21.200 kN). Then, with the weakening of the material and consequent crack growth, the force decreases and more accurate values are obtained when less number of nodes are selected, Table 5.

Fig.8a and Fig.9a clearly show that for a smaller force value $F_1$ = 15.250 kN applied at the initiation of the crack propagation, a small zone of elastic deformation is around the supports, and later (Fig. 8b and Fig. 9b) at the crack length of $d_5$ = 23.104 mm and greater force value of $F_5$ = 18.350 kN, the zone of elastic deformations is larger around the supports. Also, the size of damage affects the distribution of elastic deformations, so it can be seen that for the force value $F_1$ = 15.250 kN, the size of the elastic deformations zone below it is by far much larger than in the case of the force value $F_5$ = 18.350 kN.

Table 4. The influence of the number of nodes in supports and the number of nodes used to apply the force on calculated *J*-integral values (shaded values are closest to the experimentally obtained values).

| *J* values, N/mm $d_1$ = 16.830 mm | | Number of nodes used to apply force *F* = 15.250 kN | | |
|---|---|---|---|---|
| | | 1 | 3 | 5 |
| Number of nodes used for support | 1 | 34.26 | 33.16 | 30.98 |
| | 3 | 32.18 | 31.35 | 29.36 |
| | 5 | 28.96 | 28.72 | 26.44 |
| | 7 | 23.97 | 23.64 | 21.88 |
| *J* values, N/mm $d_2$ = 18.074 mm | | Number of nodes used to apply force *F* = 20.700 kN | | |
| | | 5 | 7 | 9 |
| Number of nodes used for support | 9 | 503.98 | 497.11 | 490.88 |
| | 11 | 389.91 | 383.77 | 377.26 |
| | 13 | 321.22 | 315.02 | 309.43 |
| | 15 | 219.87 | 214.23 | 209.02 |
| *J* values, N/mm $d_3$ = 20.009 mm | | Number of nodes used to apply force *F* = 21.200 kN | | |
| | | 5 | 7 | 9 |
| *Number of nodes used for support* | 9 | 1308.10 | 1299.90 | 1291.30 |
| | 11 | 1021.80 | 1014.10 | 1006.20 |
| | 13 | 841.99 | 833.97 | 827.67 |
| | 15 | 603.03 | 596.34 | 589.97 |
| *J* values, N/mm $d_4$ = 21.821 mm | | Number of nodes used to apply force *F* = 15.250 kN | | |
| | | 5 | 7 | 9 |
| *Number of nodes used for support* | 7 | 1011.60 | 1005.10 | 998.51 |
| | 9 | 847.26 | 840.74 | 834.35 |
| | 11 | 603.97 | 598.41 | 592.56 |
| | 13 | 466.38 | 461.12 | 456.13 |
| *J* values, N/mm $d_5$ = 23.104 mm | | Number of nodes used to apply force *F* = 18.350 kN | | |
| | | 5 | 7 | 9 |
| *Number of nodes used for support* | 11 | 1910.60 | 1901.80 | 1892 |
| | 13 | 1505.90 | 1498.40 | 1489.6 |
| | 15 | 1007.80 | 1001.20 | 994.48 |
| | 17 | 756.09 | 750.16 | 743.75 |

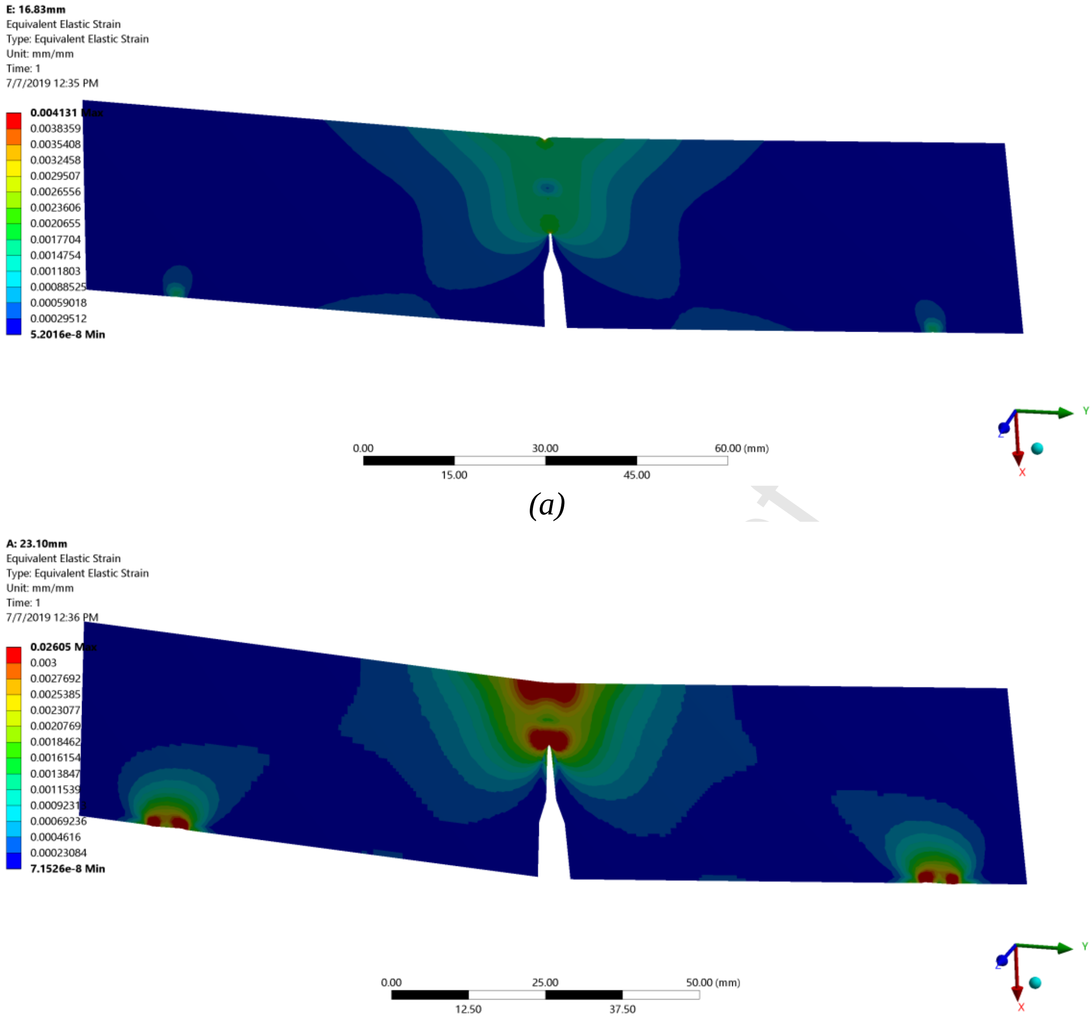


*(a)*

*(b)*

Fig. 8. The elastic deformation zones for (a) initial crack length $d_1$ = 16.830 mm and (b) final crack length $d_5$ = 23.104 mm

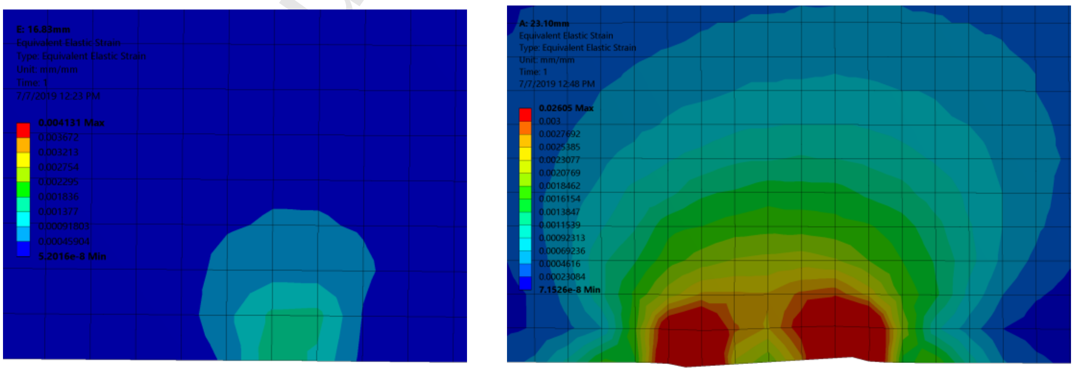

*(a)* *(b)*

Fig. 9. The elastic deformation zones at supports for (a) initial crack length $d_1$ = 16.830 mm and (b) final crack length $d_5$ = 23.104 mm

Table 5 shows a comparison between experimental and numerical $J$ values with the best approximation, and it is evident that agreements are very good.

Table 5. Comparison between experimentally and numerically obtained *J* values.

| Crack length, $\Delta a$, mm | Experimentral *J* values N/mm | Applied load, N | Best approximation of numerical *J* values, N/mm | Number of nodes |
|---|---|---|---|---|
| 16.830 | 39.14 | 15250 | 34.26 | 1 |
| 18.074 | 296.12 | 20700 | 309.43 | 13 |
| 20.009 | 608.19 | 21200 | 603.03 | 15 |
| 21.821 | 885.10 | 15250 | 847.26 | 9 |
| 23.104 | 1191.76 | 18350 | 1007.80 | 15 |

In addition, the influence of mesh density in numerical calculations of the *J*-integral is given, Fig.10, and as expected, the FEM results in case of using finer mesh are closer to experimental results.

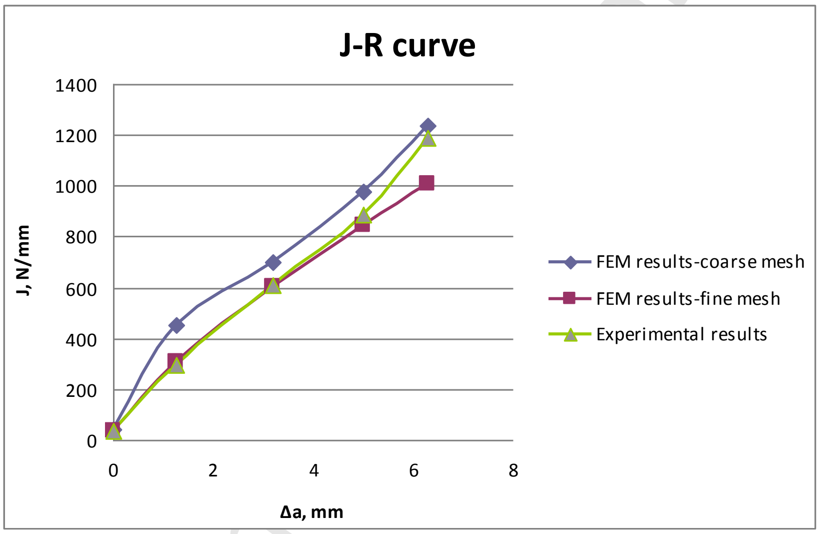


Fig. 10. Comparison of experimental specimen *J-R* curve with FEM results

The numerical analysis results also show that the numerical results of the *J* value are close to the experimental values in case of shorter cracks.

**6. Summary**

Applied techniques in this experiment enabled the evaluation of parameters important for the application of steel used on elevated temperatures. The degree of the damage to the steel steam pipelines is determined by using the local approach to ductile fracture. The critical values of the J-integral are experimentally measured on SEN(B) specimen and calculated using the FEM.

The experimental measurement of J-integral is the accurate and safest method which, due to the complexity and excessive costs, in certain cases represent a very demanding process. Numerical determination of the J-integral is nowadays reliable alternative, but some critical issues must be considered.

Firstly, to carry out acceptably accurate FEM calculations, material properties obtained in the tensile test of notched specimens must be used. Secondly, successful numerical determination of J-integral on two-dimensional FE model of specimen requires careful analysis and appropriate choice of all factors mentioned in this paper, since the presented calculated J-values show great variations. In three-dimensional FE analyses of crack growth in SEN(B) specimen (which were carried out in the research, but are not presented in this paper), modelling of elastic support rollers diminishes the need for analysis of the influence of selected nodes on the accuracy of calculated J-values, but three-dimensional FE models are demanding, have their own critical issues (for example, how to successfully model contacts) and, finally, the most important disadvantage of 3D simulation is time to final result: it is significantly longer than in a case of appropriate two-dimensional model.

Thus, it seems reasonable to additionally improve two-dimensional models and FE analysis presented in this paper, and further research will be oriented to determination of the relations between the parameters of interest, which could provide valuable information on connections among, for example, actual crack length, value of force acting on the specimen and number of nodes that should be used at supports at given instant, taking into account other standardized parameters – type of specimen, specimen dimensions, support rollers diameters, distance between rollers, etc.

To conclude, failure analysis based on J-integral values obtained numerically could be, without any doubt, very useful in engineering applications where time-saving, lower costs and high reliability are main requirements.

**Acknowledgements**

Authors acknowledge the financial support of the Serbian Ministry of Science, project TR 35011. The authors express their gratitude to Professor Milorad Zrilić from the Faculty of Technology and Metallurgy, for valuable help during experimental testing.

**References:**

[1] M. Zrilić et al., Ductile Fracture Prediction of Steam Pipeline Steel, Materials Science Forum, Vol. 518, pp. 537-542, 2006.

[2] M. Zrilić et al.,Experimental and numerical evaluation of a steamline behaviour using local approach, Metalurgija, 46(2), pp. 87-92, 2007.

[3] M. Zrilić et al., Fracture toughness and crack resistance of steam pipeline steel in initial and used states, Strength of Material, 36(1), pp. 47-58, 2004.

[4] D. Sadibašić et al., Influence of initial state on properties of MMA welded 14MoV6 3 steel, Zavarivanje i zavarene konstrukcije 2, pp. 53-60, 2012.

[5] L. Domovcova et al., Microstructure and mechanical properties of steel grade 14MoV6-3, Materials Science Forum, Vol. 782, pp. 137-140, 2014.

[6] D. Hodžić, I. Hajro, Impact toughness of steamline material 14 MoV6-3 after long-term exploitation, Proceedings of the 14$^{th}$ International Research/Expert Conference "Trends in the development of machinery and associated technology", pp. 129-132, 2010.

[7] B. Medjo et al., Micromechanical estimates of the critical values of J-integral for the steel of steam pipelines, Materials Science, 45(4), pp. 523-531, 2009.

[8] ASTM E399-17-Standard Test Method for Linear-Elastic Plane-Strain Fracture Toughness $K_{IC}$ of Metallic Materials.

[9] ASTM E1290-08e1-Standard Test Method for Crack-Tip Opening Displacement (CTOD) Fracture Toughness Measurement.

[10] ASTM E1820-18ae1-Standard Test Method for Measurement of Fracture Toughness.

[11] BS 7448-1: 1997-Fracture Mechanics Toughness Tests Part 2: Method for Determination of $K_{IC}$, Critical CTOD and Critical J Values of Metallic Materials.
[12] H. Moustbachir et al., Experimental and numerical study of stress–strain state of pressurised cylindrical shells with external defects, Engineering Failure Analysis, 17 pp. 506-514, 2010.
[13] M. Allouti et al., Study of the influence of dent depth on the critical pressure of pipeline, Engineering Failure Analysis, 21, pp. 40-51, 2012.
[14] M.A. Guidara et al., Structural integrity assessment of defected high density poly-ethylene pipe: Burst test and finite element analysis based on J-integral criterion, Engineering Failure Analysis, 57, pp. 282-295, 2015.
[15] Kim YJ et al., On experimental J estimation equations based on CMOD for SE (B) specimens, Journal of testing and evaluation; 29(1), pp. 67-71, 2001.
[16] Kirk MT et al., J and CTOD estimation equations for shallow cracks in single edge notch bend specimens, Journal of Testing and Evaluation; 21(4), pp. 228-38, 1993.
[17]C.F. Shih et al., Energy release rate along a three-dimensional crack front, International Journal of Fracture, 30, pp. 79-102, 1986.
[18]R. Akbari Alashti et al., Experimental and numerical investigation of ductile damage effect on load bearing capacity of a dented API XB pipe subjected to internal pressure, Engineering Failure Analysis, 47, pp. 208–228, 2015.
[19]Jun Hua et al., Failure analysis based on J-integral values: A case study of hydrogen blistering defect, Engineering Failure Analysis, 18, pp. 924–932, 2011.
[20] www.ansys.com

**Highlights**

- J-R curves and toughness $J_{Ic}$ of 14MoV6-3 steel have been obtained experimentally.
- 2D-FEM model based on J-integral criterion was used to analyze the defect severity.
- Special attention was paid on the influence of the mesh density, and the applied boundary conditions, to the accuracy of obtained *J*-integral values.
- Good accordance between experimental and numerical results is achieved.